2020-24-0004 Published 27 Sep 2020

Simulation Study on the Use of Argon Mixtures in the Pressurized Motored Engine for Friction Determination

Gilbert Sammut Jaguar & Land Rover

Emiliano Pipitone University Of Palermo

Carl Caruana and Mario Farrugia University of Malta

Citation: Sammut, G., Pipitone, E., Caruana, C., and Farrugia, M., "Simulation Study on the Use of Argon Mixtures in the Pressurized Motored Engine for Friction Determination," SAE Technical Paper 2020-24-0004, 2020, doi:10.4271/2020-24-0004.

Abstract

Mechanical friction and heat transfer in internal combustion engines are two highly researched topics, due to their importance on the mechanical and thermal efficiencies of the engine. Despite the research efforts that were done throughout the years on both these subjects, engine modeling is still somewhat limited by the use of sub-models which do not fully represent the phenomena happening in the engine. Developing new models require experimental data which is accurate, repeatable and which covers wide range of operation. In SAE 2018-01-0121, the conventional pressurized motored method was investigated and compared with other friction determination methods. The pressurized motored method proved to offer a good intermediate between the conventional motored tests, which offer good repeatability, and the fired tests which provide the real operating conditions, but lacks repeatability and accuracy. A 'shunt pipe' was utilized between the intake and exhaust manifolds which reduced significantly the air supply demand. In SAE 2019-01-0930, Argon was used in place of air in the experimental setup which resulted in bulk gas temperatures synonymous to the fired engine. In SAE 2019-24-0141 and SAE 2020-01-1063 mixtures between air and Argon were utilized to investigate the relationship of mechanical friction with a controlled gradual increase in the bulk in-cylinder temperature. In this publication, a one-dimensional engine model is developed to assess the capability of the 1D model to capture the effects on the motored engine imposed by changing the working gas. From the experimental studies on the pressurized motored engine, increasing the proportion of Argon to air showed an increase in the peak bulk gas temperature of around 600°C. This resulted in an increase in the heat losses, a decrease in the pumping losses and no measureable difference in the mechanical friction.

Motivation

Mechanical friction in internal combustion engines has long been studied and optimized. Further improvements in the field require the backing of an appropriate method by which reliable FMEP quantification can be made experimentally. Several of the known testing methods fall short in one or more ways in their ability to measure the FMEP with good fidelity.

The fired indicating method allows a relatively quick way of obtaining the FMEP at the actual running pressure load and thermal conditions [1]. This method however suffers from two major disadvantages, which somewhat reduces its prestige. In this method, the FMEP is obtained from a subtraction of the BMEP from the IMEP. Due to the energy released by the combustion, both the IMEP and BMEP can be an order of magnitude larger than the FMEP [2]. This implies that the uncertainty propagation on the FMEP is significant, and hence reduces the robustness of the method. Mauke [2] gives a detailed account of the present discussion of the uncertainty propagation. The other disadvantage of fired FMEP tests is that the presence of combustion induces cycle-to-cycle variability.

To address the limitations of the fired indicating method, the same procedure can be utilized on a motored engine instead. The absence of combustion yields a low coefficient of variation (COV) and the IMEP and BMEP magnitudes are brought down to values similar to that of the FMEP. As a consequence, the uncertainty propagation on the FMEP is decreased significantly. This also enables the use of torque measurement systems with a smaller range, and hence higher resolution. As discussed by Richardson [3], despite the discussed advantages, the absence of combustion results in poor representation of the actual fired conditions. These include; low pressure load, unrepresentative pressure load - to - crank angle phasing (and hence, piston velocity) and the lack of high temperature of the combustion gases.

A variant of motored testing is referred to as the 'Pressurized Motoring', or 'Motoring with External Charging' [3, 4].

This method is not a new technique, but it is claimed [2] to have been first investigated back in 1939 by Ullman [5], and later by Pike [6] in 1963. With this method, the intake manifold is pressurized with air (usually supplied from an external compressor), such that on compression stroke, the peak in-cylinder pressure (PCP) magnitude achieved is close to that of the fired engine. With this method, the IMEP and BMEP magnitudes are still small and comparable to that of the FMEP; hence the small uncertainty propagation advantage is retained, whilst giving some pressure load representation on the FMEP.

Despite the ability of the pressurized motored method to reach fired-like peak in-cylinder pressures, the pressure load - to - crank angle phasing still differs from that of the fired engine, as shown clearly by Mauke [2] and Allmaier [4]. Another shortcoming of the conventional pressurized motoring (i.e. using air as the working gas) is that the method is not capable of inducing high gas temperatures [3]. In [7] the pressurized motoring method was improved by utilizing gases of ratio of specific heats higher than that for air. This results in fired-like in-cylinder temperatures, which therefore emulates better any thermal expansions of the piston, piston rings and piston pin, as well as emulate any oil film degradation due to the high in-cylinder temperatures.

The conventional pressurized motoring (using air) is claimed to be mainly useful when its measured FMEP is compared against fired FMEP data acquired at the same engine operating point of speed and pressure load [1, 4]. The reason for this is discussed at greater length in forthcoming sections. While matching the engine speed between the fired and pressurized motored testing is easy, matching pressure load is debatable. In research by MAHLE [1] and Allmaier [4], the pressure load on the piston and cranktrain was matched by setting the PCP equal for both fired and pressurized motored tests. Mauke [2], however, explains that due to differences in the pressure load-to-crank angle phasing between the two methods, the fired pressure load throughout the entire cycle is better represented by the pressurized motored method if the same integral lateral piston force is present over the high-pressure stage of the cycle, by selecting a suitable (calculated) charge pressure. Therefore, with the method brought forward by Mauke [2], the PCP between the fired and pressurized motored testing might not necessarily be equal.

Experimenters are in search of methods which are able to measure the "global" and "component" FMEP with good fidelity, but which are (possibly) also capable of capturing all the fired effects on the FMEP measurement. Due to the absence of faithful FMEP measurements, predictive one-dimensional simulation still makes use of traditional FMEP sub-models of the Chen-Flynn type. This predicts the FMEP based on the engine speed, magnitude of peak in-cylinder pressure, windage losses and accessory losses. This model therefore is not capable of capturing any variation in FMEP contributed from the thermal load, and pressure load phasing with crank angle. As a result it is thought that the modified form of the pressurized motored method presented in [8], [9] and companion paper [10] may be utilized as the basis for development of new friction sub-models (or modifying existing ones). Publications [8] and [9] focus on the thermal load contribution on the FMEP, whereas [10] focuses mainly on the pressure load to crank angle phasing contribution on the FMEP.

Introduction

The bulk gas temperature in motored engine operation is mainly dependent on the compression ratio, intake gas temperature and the polytropic index [4]. If the intake manifold temperature is constant, it can be shown that the bulk gas temperature in the pressurized motored method is *relatively* insensitive to engine speed and load. This gives the possibility of measuring the FMEP at different engine speeds and mechanical loads, independently from in-cylinder thermal conditions [1]. This quality is particularly useful when analyzing the FMEP contribution of new component designs. MAHLE [1] used the pressurized motored engine (conventionally with air) for this temperature decoupling characteristic, to determine the FMEP reductions due to several optimizations on the piston and ring-pack. Testing was done on both the pressurized motored engine, and the fired engine at the same engine speed and peak in-cylinder pressures. The differences obtained in the FMEPs between the two methods were attributed to the different thermal effect. Using the pressurized motored engine with air offers the discussed temperature decoupling effect, however the in-cylinder temperature cannot be controlled by the experimentalist.

In [8] and [9] a modification was proposed to the conventional pressurized motoring method, where mixtures of air and argon at different concentrations were used to pressurize the intake manifold. This method retained the temperature decoupling effect synonymous with the conventional pressurized motored method, and in addition gave the experimentalist the flexibility of controlling the temperature independently from other control variables, by utilizing the appropriate mixture of air to argon. This is considered of benefit if the temperature contribution on the FMEP is being investigated.

The work performed so far by the authors investigated the conventional method of pressurized motoring using air in [11]. A shunt pipe was introduced between the intake and exhaust manifolds to recirculate the air, with the aim of reducing the need of a large external compressor. In [7], the addition of pure Argon was investigated experimentally and proved able to increase the peak in-cylinder temperatures. An amendment to the setup was done whereby the blow-by was also recirculated back to the intake via a small compressor, which further decreased the size of the external pressurization supply required. In [8], the already mentioned experimental study using Argon-to-air mixtures were performed with the aim of studying the FMEP dependency on bulk gas in-cylinder temperature. In [9], Argon-to-air mixtures were also investigated at a higher PCP. Apart from the FMEP, preliminary work on experimental heat flux was also presented. In [12], a simulation study was conducted which correlated a one-dimensional model with the experimental data obtained from the pressurized motoring using air. In the companion paper [10], a novel modification to the pressurized motoring method was proposed with the aim of obtaining a versatile method with high degrees of freedom to allow developments of novel FMEP models. The novel method is referred to as the 'pressurized fuelled motoring' with which the pressurized motoring method using air can be improved through the addition of small injection quantities of fuel. Motoring of the engine and

gas recirculation are still retained. This method was shown to be feasible, according to the simulation study. The method gives the versatility of a very large degree of freedom, where the in-cylinder pressure (magnitude and phasing) and the in-cylinder temperature can be made to emulate the fired conditions to a very good extent. The FMEP measurement accuracy is also enhanced. It was found however that all these qualities cannot be achieved together in the same test; but several conditions can be tested individually to characterize the FMEP of the fired engine. The pressurized fuelled motored method is mentioned throughout this paper; however it is not the scope of this paper to discuss this method. Hence, discussion is limited to some references and comparisons. Results from the companion paper [10] are given where necessary throughout this paper for ease of reference.

The simulation work put forward in this publication is aimed at developing a one-dimensional model to represent the engine working on Argon and its mixtures with air, as tested experimentally in [7], [8] and [9]. This is done with the aim of understanding whether a simulation model can be correlated to the experimental data using working gases other than air, whilst giving a better insight to the Argon method. A similar simulation study was already done and communicated in [12], however the engine simulation software used in that publication did not allow the use of Argon, and hence the simulation had to be limited to pressurized motoring with air only. It was concluded in [12] that the one-dimensional model reaches a relatively good correlation with the experimental data for pressurized motored operation with air, however the crank angle resolved heat transfer, as estimated using Annand and Woschni models resulted in a relatively different shape to what was obtained experimentally. The FMEP as predicted from the Chen-Flynn also showed some differences when compared to the experimental data.

In the forthcoming sections, the main focus will be on mechanical friction and in-cylinder bulk gas temperature; however other parameters will also be discussed.

Simulation Model

The simulation model studied in this work was built in "GT-Suite", which is a commercial software used for one-dimensional thermo-fluid engine analysis [13]. In developing the model, the geometry for the 2.0 HDi engine (shown in Table 1) tested experimentally in [11, 7, 8, 9], and also simulated in [12] and the companion paper [10] was used. Only one cylinder was modeled to reflect the experimental engine configuration at the time of writing. Table 1 gives the specifications of the engine studied.

To reflect the actual experimental setup, the simulation model was also assigned with a shunt pipe between the intake and exhaust manifolds. The shunt pipe was used initially in [11], with air as the working gas. It proved to be a good method of how the supply flow rate of air in pressurizing the system can be kept to a minimum, and manageable with a conventional compressor [11]. Figure 1 shows a schematic of the experimental setup which this simulation emulates. It should be noted that in [7], [8] and [9], when Argon and its mixtures with air were used, the shunt pipe proved to be very beneficial, since the relatively expensive gas was not consumed, but re-circulated. To reduce further the gas supply mass flow rate, the crankcase breathers of the engine were ducted to a small, variable speed reciprocating compressor, and they were pressurized back to the intake manifold through an oil trap. Testing the engine at a reasonable sized experimental test matrix reaching thermal steady state, could be sustained from a pressurized 10 Nm^3, 200 bar Argon cylinder. In the simulation model presented, engine blow-by was not modeled.

The model developed in this work was configured to operate in the motored mode. Argon gas properties were already available in GT-Suite. The software supported investigation of Argon mixtures with air, which allows modeling of the experimental studies such as those conducted in [8] and [9] by the same authors, and in [15] by Demuynck. Due to setting the simulation in motoring, the only sub-models

TABLE 1 Engine specifications [14]

Make and Model	Peugeot 306 2.0L HDi
Year of Manufacture	2000
Number of Strokes	4-stroke
Number of Cylinders	4, active 1
Valvetrain	8 Valve, OHC
Static Compression Ratio	18:1
Engine Displacement [cc]	1997
Bore [mm]	85
Stroke [mm]	88
Connecting Rod Length [mm]	145
Intake Valve Diameter [mm]	35.6
Exhaust Valve Diameter [mm]	33.8
Intake Valve Opens (1mm lift)	10 CAD ATDC intake
Intake Valve Closes (1mm lift)	20 CAD ABDC intake
Exhaust Valve Opens (1mm lift)	45 CAD BBDC expansion
Exhaust Valve Closes (1mm lift)	10 CAD BTDC exhaust

FIGURE 1 The pressurized motored experimental setup schematic.

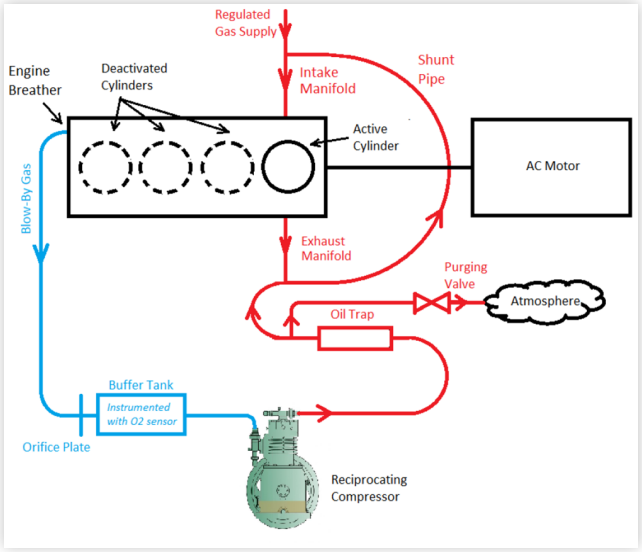

required to be assigned were those for the heat transfer, and mechanical friction.

The heat transfer model utilized was a modified form of the Woschni model. The Woschni model was chosen since it was developed on both motored and fired engines, as dictated by Finol [16]. Hence it is thought to be able to represent better the pressurized motored engine. Ports and cylinder wall temperatures were not imposed but calculated by a wall temperature solver. The external coolant side heat transfer coefficient was made proportional to the engine speed. The internal heat transfer coefficient for the ports was predicted using the Colburn analogy.

The simulation software used in this work only allowed the use of the Chen-Flynn model for estimation of the mechanical friction. This model uses one set of user-defined coefficients which are applied at all the simulated conditions.

In the forthcoming sections, the results obtained from the simulation are presented and discussed. The simulation was run at two engine speeds of 1400 rpm and 3000 rpm, with varying PCPs between 80 bar and 160 bar. The gas composition was also varied from 100 % air (0% Argon) to 100 % Argon. The results section of the publication is split up as follows:

Part I: The simulation results for the engine speed of 1400 rpm are presented and discussed. These aim to determine whether the simulation model is able to represent the pressurized motored engine utilizing different gases. Maximum and minimum values for the two engine speeds investigated are given at the end of the section.

Part II: The simulation results obtained at the engine speed of 1400 rpm are compared with those of the conventional pressurized motoring using air, and the fully fired engine. Crank angle resolved metrics are also presented and compared.

Simulation Results - Part I: Fixed Engine Speed, Varying PCP and Argon Mass Fraction

It was noted that the parameters of interest in this study showed similar behaviors with Argon mass fraction and PCPs, at the two simulated speeds. For the sake of conciseness, the results presented and discussed in this section are those obtained at 1400 rpm, unless stated otherwise.

To aid in the discussion which follows, gas properties for air and Argon are given in Table 2. It should be made clear, that in this study, the aim was to simulate the engine with gases of different ratio of specific heats. However, changing the gas does not just change the ratio of specific heats, but also changes significantly other parameters, as shown in Table 2.

In the following sub-sections, several metrics of interest are presented and discussed, with particular focus on their relationship with the Argon mass fraction as a mixture with air. Experimentally determined values published in [8] and [9] are given at the corresponding conditions of PCP and argon concentration to assess the correlation of the one dimensional model with the experimental data. The color within the experimental markers (circles) is aimed to visually indicate the magnitude of the experimental value. It should be noted that in [8] and [9], the Argon mass fractions tested were 0 %, 57 %, 87 % and 100 %. These values correspond to ratios of specific heat of 1.40, 1.50, 1.60 and 1.67.

Intake Manifold Pressure

The intake manifold pressure is given in Figure 2. The discrete points superimposed on Figure 2 at 84 bar and 103 bar are the experimentally measured values from [8] and [9]. It is noticed that the intake manifold pressure (or equivalently, shunt pipe pressure) decreases with an increase in the Argon mass fraction. This observation is consistent with the

FIGURE 2 The contour of intake manifold absolute pressure at 1400 rpm.

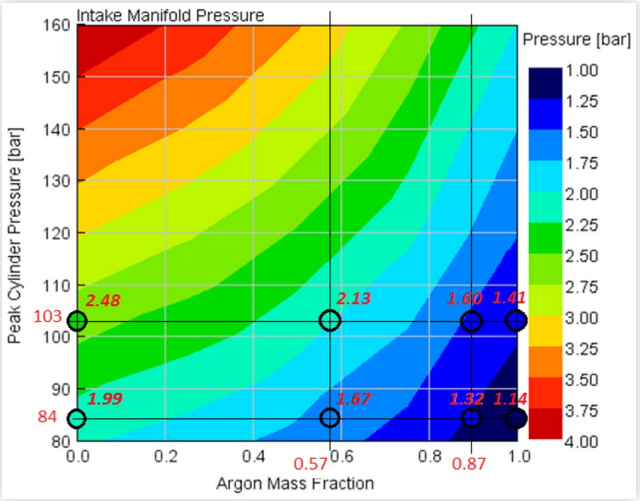

TABLE 2 Properties of air and Argon at two different temperatures [15, 13].

		Density [kg/m^3]	Ratio of Specific Heats	c_p [J/kg.K]	c_v [J/kg.K]	Dynamic viscosity [Pa.s]	Thermal Conductivity [W/m.K]
298 K	Air	1.184	1.40	1000	718	1.90e-5	0.026
	Argon	1.634	1.67	520	312	2.27e-5	0.018
900 K	Air	0.394	1.34	1100	834	3.90e-5	0.063
	Argon	0.541	1.67	520	312	5.17e-5	0.040

experimental results, and can be intuitively understood through a theoretical analysis using the polytropic equation, referenced to IVC conditions, and given by equation (1), where n is the polytropic exponent and varies depending on the gas composition and the engine operating setpoint. It can be shown that using gases with higher ratio of specific heats results in the same PCP, but with a lower manifold pressure.

$$p_{max} = p_{IVC}\left(\frac{V_{IVC}}{V_{@p_{max}}}\right)^{n} \quad (1)$$

Figure 2 also shows an increase in the intake manifold pressure with an increase in the peak in-cylinder pressure. This is expected and consistent with theoretical expectations, meaning that achieving a higher PCP in the conventional pressurized motoring can be done through an increase in the intake manifold pressure, and a consequent increase in the cylinder trapped mass. The simulation results show deviations of around 6% at the experimental test points.

Manifold Temperatures

The shunt pipe attached between the intake and exhaust manifolds was simulated with a wall temperature solver. External heat exchange to ambient was assigned an arbitrary 20 W/m^{2}K convection coefficient to a 320 K sink temperature. Radiation component of heat transfer was also assigned with the same 320 K sink temperature. The internal convective heat transfer coefficient assigned to the shunt pipe made use of the "Colburn analogy". The manifold temperatures that resulted in the intake and exhaust manifolds are presented in Figure 3 and Figure 4 respectively. Discrete experimental results from [8] and [9] are also encircled in the same figures. A white color is used in the experimental markers due to their magnitude which falls outside the range of the figure legend (by around 10 - 20 °C).

Figure 3 and Figure 4 both show an increase in temperature with an increase in PCP, and decrease in Argon content.

FIGURE 3 The contour of intake manifold temperature at 1400 rpm.

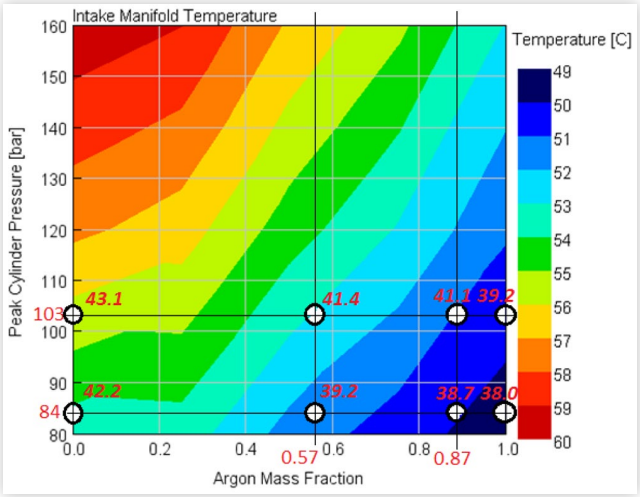

FIGURE 4 The contour of exhaust manifold temperature at 1400 rpm.

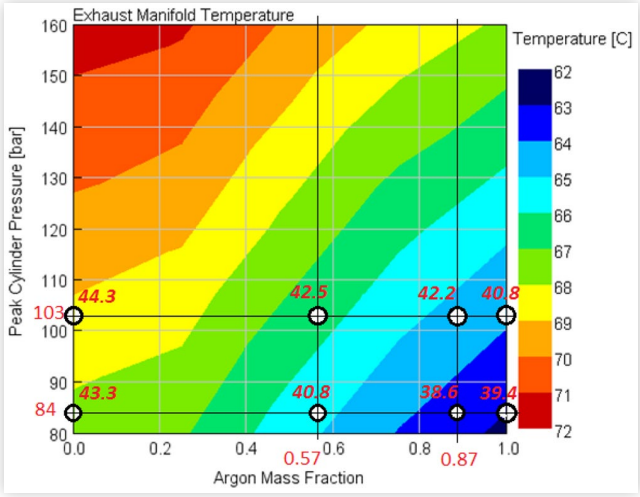

The two relationships are somewhat related, and attributed to the recompression occurring during the exhaust stroke, and heat transfer from the cylinder. The relationship of temperature with recompression is discussed in the following text.

In a motored engine, the heat and blow-by losses act to reduce the pressure, and consequently the temperature of the in-cylinder gases throughout the closed part of the cycle. This means that the in-cylinder pressure and temperature at EVO are lower than the in-cylinder pressure and temperature at IVC. However, with the use of the pressurized motoring method using the shunt pipe, it was observed experimentally in [11, 7, 8, 9], and with simulation in Figure 3 and Figure 4, that the temperatures of the gases at the exhaust manifold are higher than the temperatures at the intake manifold. This result was confirmed by the simulation in the companion paper [10] and attributed to two processes which occur at EVO that increase the temperature of the exhaust gases to values higher than those of the intake gases. The two processes are explained in the subsequent text, and their result is shown graphically in Figure 5.

The first process is that upon EVO, gas from the shunt pipe rushes into the cylinder to achieve pressure equilibrium between the shunt pipe and the cylinder. This can be thought

FIGURE 5 The in-cylinder gas pressure and temperature (using air) with a range of increasing exhaust valve area.

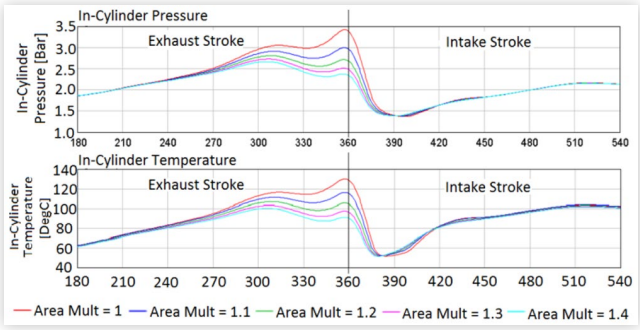

of as an opposite process to what is conventionally known as 'blow-down' in fired engines. The second process occurs during the displacement phase, where the exhaust flow is restricted by the exhaust valve curtain area. This creates a recompression of the gases which therefore increase both the pressure and temperature of the exhaust gases, over that of the intake gases. The simulation in the companion paper [10] confirmed these two processes by assigning multipliers to the exhaust valve curtain area, as shown in Figure 5. Results showed that the smaller the area, the larger will be the in-cylinder exhaust gas pressure and temperature.

Figure 3 and Figure 4 show an increase in temperature with an increase in PCP. This is due to the fact that a higher PCP is obtained with a larger quantity of trapped mass, hence the restrictive exhaust valve curtain area will have an even greater effect.

Even though not shown here, the intake and exhaust manifold temperatures for the case of 3000 rpm, reached maxima of 95 °C and 111 °C respectively, which are both higher than the maxima for the 1400 rpm, communicated in Figure 3 and Figure 4. This is also related to the explanation given above, since a higher engine speed allows less time for the gases to flow out of the exhaust valve, and hence the curtain area restriction becomes more prominent.

This variation in the intake manifold temperature with engine speed consequently results in some variation in the peak in-cylinder bulk gas temperature with engine speed. This might seem contradicting to previous claims made in the paper. It should however be pointed out that the differences in peak bulk gas temperature that were noted experimentally in [8] and [9], across a test matrix from 1400 rpm to 3000 rpm is at a maximum of 150 DegC, which is small compared to the increase in the peak bulk gas temperature increase with changing the gas composition, as shall be seen in a later figure (Figure 8). Additionally, external conditioning of the intake gas using a heat exchanger can be carried out to eliminate these unwanted variations. This however was deemed detrimental by the authors due to the associated complication in modeling the heat exchanger due to wave reflections and other fluid transport phenomena - hence was never implemented on the experimental setup.

Figure 3 and Figure 4 show that increasing the Argon content decreases the manifold temperatures. This was also noted experimentally in [8] and [9], but to a lesser extent, as shown by the experimental markers. This observation can be explained by considering the earlier Figure 2, which showed that to achieve a certain PCP, increasing the Argon content results in a decrease in the manifold pressure. As a result, an increase in the Argon content results in a decrease in trapped mass, which alleviates slightly the restriction problem of the exhaust valve curtain area, as shown in Figure 6. Due to the smaller recompression, the resulting manifold temperature is lower.

Location of Peak In-Cylinder Pressure

It was discussed that the pressurized motoring method obtains high PCPs due to an appropriate trapped mass, which provides

FIGURE 6 The in-cylinder pressure during the exhaust and intake stroke for air and argon operation at 3000 rpm, 80 bar.

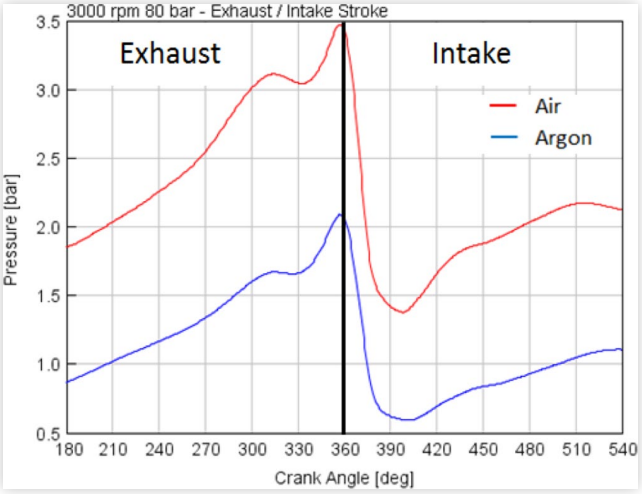

a peak in-cylinder pressure similar in magnitude to that of the fired engine. It is noted however that for motored engine operation, the peak in-cylinder pressure occurs just before TDC [17]. This is shown in Figure 7, where the simulation LPP varied between - 0.2 DegCA and - 1.5 DegCA. The experimental markers show a variation in LPP between -0.7 DegCA and -1.6 DegCA. It is also noticed that increasing the Argon content advanced the LPP to earlier crank angles, as seen experimentally in [7, 8, 9]. This is mainly due to the heat losses which are expected to get larger with increasing the Argon content. In the present study, the LPP trend is important as it gives a convenient indication of the pressure phasing with crank angle; something which is thought to be important for a representative FMEP determination. The FMEP, which is one of the main parameters of focus in this study is not just dependent on the LPP, but on the whole pressure cycle.

At Argon concentrations higher than 50 %, the simulation results in Figure 7 shows that increasing the PCP for the same Argon content, retards the LPP closer to TDC. This is expected, and was also observed experimentally in [7]. The experimental

FIGURE 7 The contour of LPP at 1400 rpm.

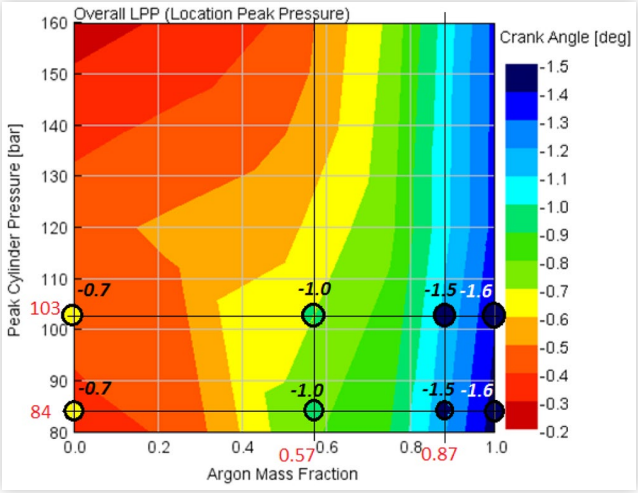

data obtained in [8] and [9], and presented by the experimental markers in Figure 7 show minimal difference (2nd digit of precision - not shown) in LPP between the two different PCPs. At Argon concentrations lower than 50 %, the relationship reported by the simulation between LPP and PCP is not well understood. Refining the model timestep resolution might give a better prediction of the LPP.

In-Cylinder Temperature and Heat Transfer Rate

The bulk gas peak in-cylinder temperature obtained from simulation is given in Figure 8. The discrete experimental results obtained in [8] and [9] are also given. The experimental results are calculated values using the ideal gas law referenced to IVC, and making use of the measured in-cylinder pressure. It is noticed that the simulation peak in-cylinder temperature shows an increase of around 1000 °C from 100 % air (0 % Argon) to 100 % Argon. This increase in temperature shows that the use of a gas with a high ratio of specific heats has the ability of increasing the peak in-cylinder temperatures to values which are close to that of the fired engine. The crank angle resolved bulk gas temperature obtained in pressurized motoring using Argon is compared to the fired gas temperature in a forthcoming section. The simulation peak bulk gas temperature does not show a good correlation with the experimental results given in the same Figure 8. Up to around 40 % difference is evident. This could have originated from a non-representative heat transfer sub-model in the simulation and due to deviations between the experimental and simulation intake manifold temperature (as shown in Figure 3).

Another observation made from Figure 8 is that the peak in-cylinder temperature stays relatively constant with an increase in PCP. This is something which is expected and can be intuitively understood through the polytropic equation written in terms of the temperature, as given in equation (2). The property of having a relatively constant peak in-cylinder temperature (and crank-resolved temperature trace) at

FIGURE 8 The contour of overall peak in-cylinder temperature at 1400 rpm.

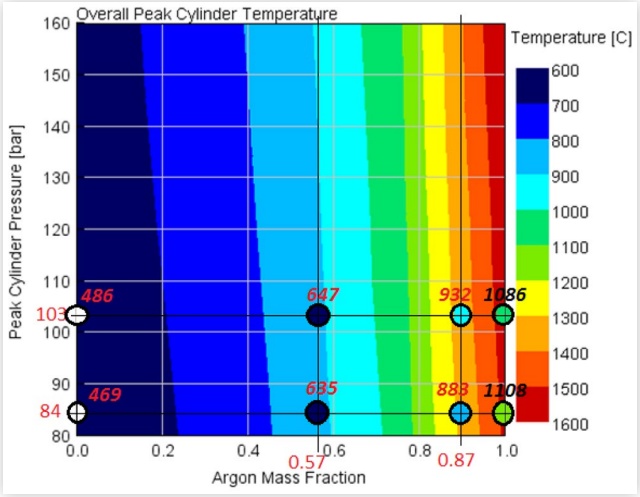

FIGURE 9 The contour of average heat transfer rate at 1400 rpm.

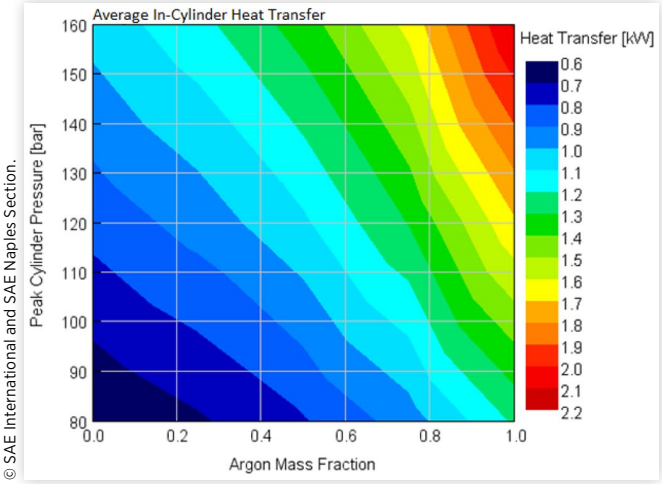

different PCPs and engine speeds is the principal motivation for using the pressurized motored method. With Argon mixtures, this quality is enhanced further by allowing the peak bulk gas temperatures to be set at the desired values, which can range from low motoring magnitudes to high fired magnitudes. Hence, the experimental measurement of the FMEP can be done at different loads and engine speeds but at a similar in-cylinder temperature trace of the experimenter's choice. This ability of decoupling between mechanical load and in-cylinder temperature allows for a better understanding of their individual contributions on FMEP.

$$T_{max} = T_{IVC}\left(\frac{V_{IVC}}{V_{@T_{max}}}\right)^{n-1} \quad (2)$$

The simulation average in-cylinder heat transfer rate, as computed from the modified Woschni correlation is given in Figure 9. It is shown that increasing both the PCP, and the Argon content resulted in an increase in the heat transfer rate, which is expected and also intuitive. Further comments on the heat transfer in the pressurized motored engine are made in a forthcoming section where the crank-angle based heat transfer from the pressurized motored engine is compared with that for a fired engine.

Mean Effective Pressures

The indicated mean effective pressure over the full 720 DegCA is given in Figure 10, together with the corresponding discrete experimental results obtained from [8] and [9]. For motored engine operation, due to the absence of combustion, the mean effective pressures represent just losses from the engine. In particular, the IMEPnet given in Figure 10 represents the heat losses, blow-by losses and pumping losses. As stated in an earlier section, blow-by was not modeled in this simulation study.

Comparing the simulation IMEPnet to the experimentally measured values show relatively good correlation with the maximum variation reaching 23 % for the condition of 0 % Argon, 84 bar PCP.

FIGURE 10 The contour of IMEPnet at 1400 rpm.

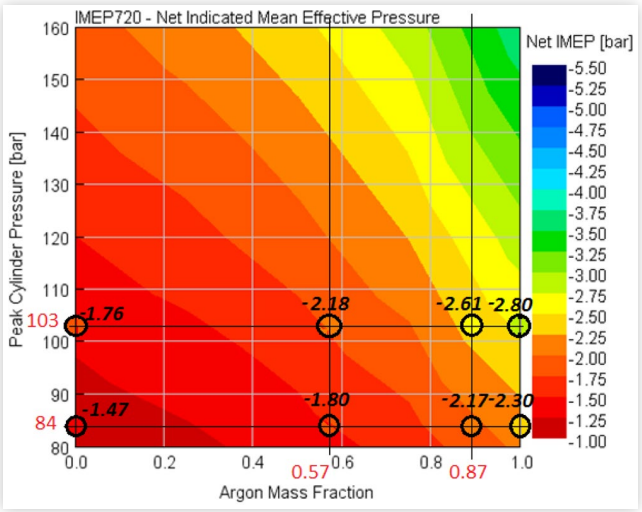

It is shown that increasing the Argon content results in an overall increase in the IMEP losses. This is mainly due to the higher heat losses induced by the elevated in-cylinder temperatures. A higher loss is also noted with an increase in PCP.

The pumping losses are given in Figure 11. It is shown that increasing the Argon mass fraction from 0 % to 57 % results in an increase in the PMEP losses. Increasing further the Argon mass fraction to 100 % resulted in a decrease in the PMEP losses. The experimental results of the PMEP obtained from [8] and [9] are also included with circle markers in the same figure, which show the same trend as the simulation data. It is understood that a gas with a higher ratio of specific heats result in the same PCP with a smaller trapped mass. As a consequence, the PMEP losses should steadily decrease with an increase in Argon content. The resultant trend shown in Figure 11 might have resulted from conflicting effects on the PMEP imposed by other external factors, such as gas properties. At present the authors refrain from attempting to explain this relationship further. Figure 12 shows the pumping loops for air and Argon operation at 3000 rpm, 80 bar PCP. This particular high speed setpoint was chosen to highlight also the difference in the recompression between air and argon operation.

FIGURE 12 The pumping loops for air and argon operation at 3000 rpm, 80 bar.

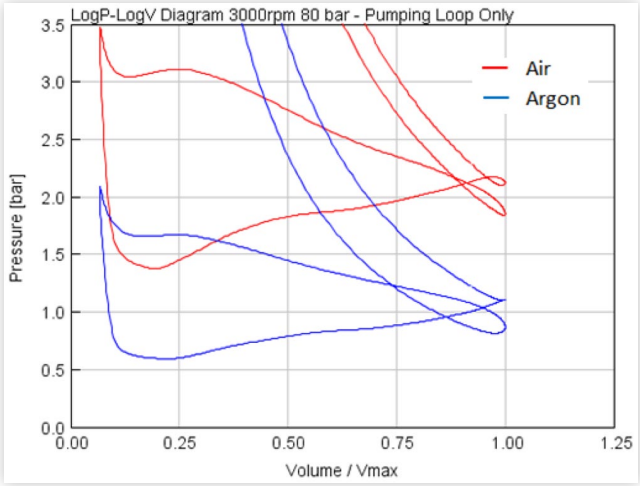

Figure 11 also shows that the pumping losses increase with an increase in PCP. Similar to the previous observation, this can be understood from the fact that with pressurized motoring methods, the PCP is obtained through an appropriate trapped mass. Hence, a higher PCP requires a higher trapped mass, and consequently a higher PMEP loss. Figure 11 shows that a relatively good correlation is evident between the simulation values and experimental measurements, with maximum deviation of around 12 %.

The total losses of the engine are represented by the BMEP, as given in Figure 13. The experimental results recorded in [8] and [9] are given in the same figure, with very good

FIGURE 11 The contour of PMEP at 1400 rpm.

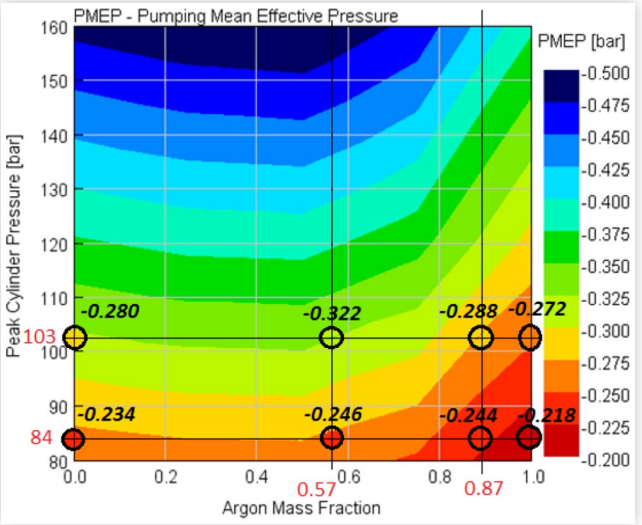

FIGURE 13 The contour of BMEP at 1400 rpm.

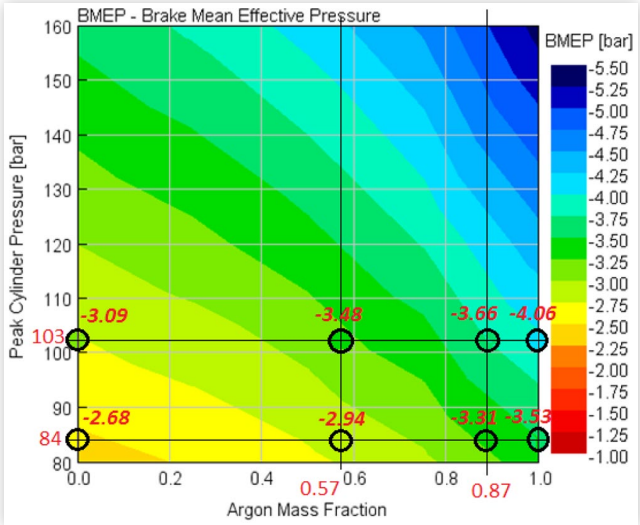

correlation. A maximum deviation of 11 % was seen at 103 bar PCP and 0 % Argon.

Obtaining the BMEP from the IMEPnet requires the addition of the FMEP losses to the IMEPnet losses. The Chen-Flynn FMEP model used in this study predicts that at the different Argon contents, the FMEP stays constant - meaning that it is insensitive to temperature. This is expected on inspection of the Chen-Flynn model equation. On the other hand, the FMEP model shows a proportional increase with an increase in PCP. As a result, it should be pointed out that the FMEP, as computed from the Chen-Flynn model was only used to have an approximate value of the BMEP. It is however stressed that the FMEP as given by the model is not sensitive to the thermal load of the engine, and hence is of limited use in this study. Even though not shown here, the FMEP was predicted by the sub-model to vary between 1.30 bar and 1.70 bar for the engine speed considered here, i.e. 1400 rpm.

Power Losses

To give a tangible value for the experimenter looking to implement the Argon method, Figure 14 was plotted which shows the power delivered by the electric motor (driver) in sustaining the operation at the discussed engine speed and PCPs. It is noted that a maximum power requirement of 3.1 kW is predicted at 1400 rpm and 160 bar using 100 % Argon. It was also predicted that at the higher simulated speed of 3000 rpm (not shown here), the brake power required reached a maximum value of 5.9 kW at 103 bar, and 8 kW at the 160 bar condition. It should be reminded that these values are pertinent to the single cylinder engine; however it is thought that such power requirements are insignificant for typical engine testing. For the four-cylinder experimental engine running at 3000 rpm, 103 bar PCP and using 100 % Argon, the power delivered by the electric motor was measured to be equal to 21 kW [9], hence an error of 12 % exist in the simulation prediction.

FMEP Robustness Factor

As described in an earlier section, one of the main advantages of using a motored method is the ability to allow a measurement of the FMEP with very small uncertainty propagation due to the absence of combustion. In the companion paper [10], a metric was introduced and defined by equation (3), where the FMEP is compared to the dominant value between IMEPnet and BMEP. Hence, the higher the FMEP robustness factor is, the lower the uncertainty propagation on the FMEP. Figure 15 gives the FMEP robustness factor for the pressurized motoring ranging from air to Argon. It can be noticed that the pressurized motoring method using air (0 % Argon) offers the highest FMEP robustness. Utilizing a higher Argon mass fraction and increasing the PCP deteriorates the FMEP robustness factor.

$$FMEP\ Robustness\ Factor = \frac{FMEP}{\max\left(abs\left(IMEPnet\right), abs\left(BMEP\right)\right)} \quad (3)$$

Other Engine Speed

In the previous sections the results for the 1400 rpm condition were presented. Table 3 gives the maximum and minimum values for the already presented 1400 rpm, and also for the other simulated engine speed of 3000 rpm. It should be noted that the minimum (or maximum) of one metric does not necessarily coincide with the minimum (or maximum) of another metric. Table 3 is aimed at giving the overall range for each parameter expected when operating with different gases ranging between 100 % air (0 % Argon) to 100 % Argon.

FIGURE 14 The contour of electric motor (driver) power at 1400 rpm.

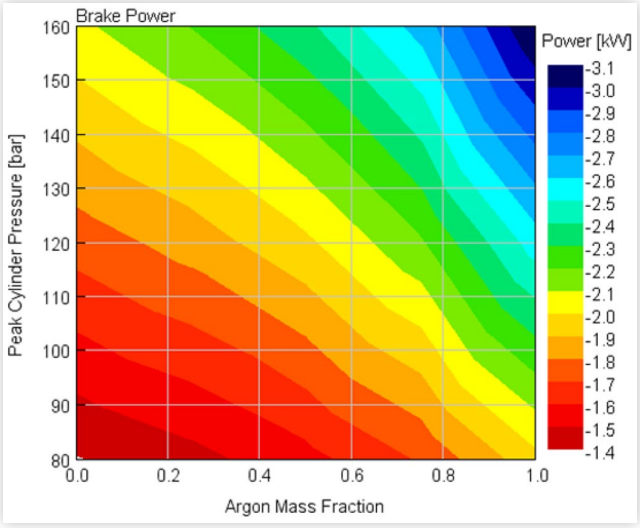

FIGURE 15 The contour of FMEP robustness factor at 1400 rpm

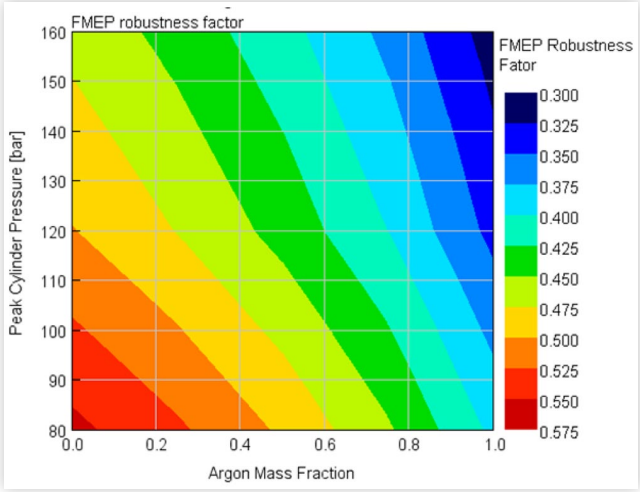

TABLE 3 The minimum and maximum values of the 1400 rpm and 3000 rpm engine speed conditions

			Min	Max	Min	Max	Min	Max
	Engine Speed	rpm	1400		3000		1400	3000
1	LPP	deg aTDC	-1.5	-0.2	-1.5	-0.4	**-1.5**	**-0.2**
2	Max Cylinder Temperature	C	600	1600	600	1600	**600**	**1600**
3	Intake Manifold Pressure	bar abs	1.00	4.00	0.75	4.00	**0.75**	**4.00**
4	BMEP	bar	-5.50	-2.50	-6.50	-3.50	**-6.50**	**-2.50**
5	IMEP720	bar	-3.75	-1.00	-4.25	-1.50	**-4.25**	**-1.00**
6	FMEP	bar	1.30	1.70	1.80	2.20	**1.30**	**2.20**
7	PMEP	bar	-0.50	-0.20	-1.70	-0.60	**-1.70**	**-0.20**
8	FMEP Robustness Factor		0.30	0.58	0.30	0.55	**0.30**	**0.58**
9	Brake Power	kW	-3.10	-1.40	-8.0	-4.3	**-8.0**	**-1.4**
10	In Cylinder Heat Transfer Rate	kW	0.6	2.2	1.4	4.4	**0.6**	**4.4**
11	Exhaust Manifold Temperature	C	62	72	95	111	**62**	**111**
12	Intake Manifold Temperature	C	49	60	60	95	**49**	**95**

Simulation Results - Part II: Comparison between Pressurized Motoring Using Air, Pressurized Motoring Using Argon, and Fired Operation

The results presented in the previous section show that the pressurized motored method using Argon mixtures, in some aspects provides enhanced data quality over the pressurized motoring using air. This is due to the Argon method having the ability to obtain fired-like peak in-cylinder temperatures, as well as a representative PMEP. This gives the ability of measuring the FMEP with a closer representation of the fired engine, whilst still retaining a good FMEP robustness factor.

This section is aimed at presenting some comparative analysis, also obtained through simulation, which compares several parameters of interest between the pressurized motoring using air, the pressurized motoring using Argon, and the fully fired engine (fired indicating method). The fired engine simulation was calibrated against the full load operation of the same 2.0 HDi engine, as tested in [11]. In this section the PCP was made to vary from 50 bar to 100 bar to include the range of PCP studied in the experimental measurements in [8, 9], and in the other simulation results reported in [12], and in the companion paper [10].

In-Cylinder Pressure

It was discussed at length by Mauke [2] that the FMEP is greatly dependent on the lateral thrust between the piston and the cylinder. Mauke [2] argues that when the pressurized motored method (using air) is run at the same peak in-cylinder pressure of the fired engine, the FMEP representation obtained from the pressurized motored engine is not satisfactory. The author states that this is due to the different phasing between the pressure load and the piston velocity of the two methods. To better this representation, Mauke [2] puts forward the 'Integral Lateral Force method', which sets the peak in-cylinder pressure of the pressurized motored engine at a value which gives the closest overall lateral thrust when compared to the operating condition of the fired engine.

It is the authors' opinion that the concern put forward by Mauke [2] is one of great importance for the field of FMEP study. This is actually taken further, and hypothesized that the FMEP dependency on pressure load-to-piston velocity relationship might also be affected by the in-cylinder temperatures and lubrication viscosity, especially where hydrodynamic conditions prevail.

To depict better the foregoing discussion, Figure 16 is plotted, which provides a comparison between the in-cylinder

FIGURE 16 The comparison of in-cylinder pressure between firing, motoring using air and motoring with Argon, at the same engine speed of 1400 rpm and PCP of 80 bar

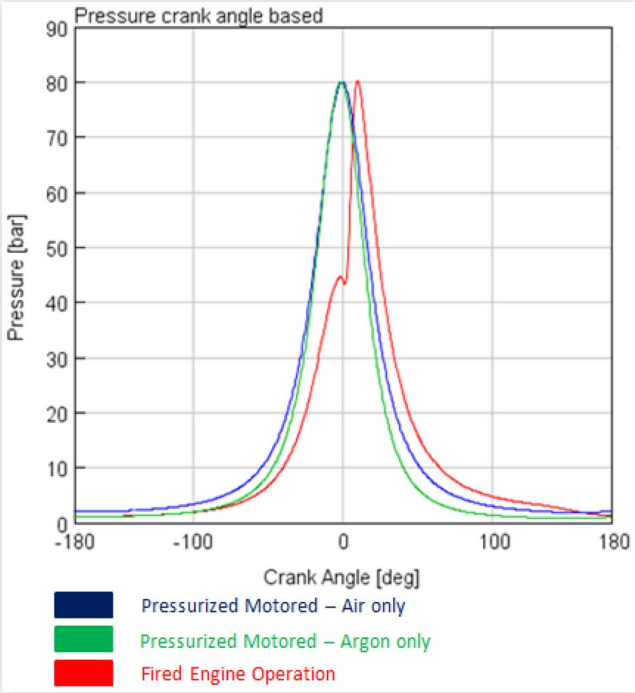

pressure obtained with pressurized motoring using air, Argon and the fired engine. It is shown that, as stated earlier, the peak in-cylinder pressure for the motoring methods are obtained at an earlier crank angle than the fired engine. It is also noted that on the compression stroke, the in-cylinder pressures of the pressurized motored methods are higher than that of the fired engine. This is due to the fact that in fired operation, the combustion acts to increase the in-cylinder pressure from the small compression pressure to the target PCP, whereas the motored methods achieve their PCP just by trapping a higher gas mass.

On the expansion stroke, it is noted that the pressurized motored methods show a consistent lower pressure than the fired engine, with the Argon case showing the lowest pressure. This can be explained by the larger heat losses incurred with the Argon case (compared to that with air), as well as the smaller induced mass during the intake stroke. It is thought that if a gas with a lower ratio of specific heats than that of air is used, the expansion stroke pressure might be closer to that of the fired case. However it is expected that the compression stroke will then suffer from a higher discrepancy from that suffered by the Argon gas. It is noted that exhaust gases have a ratio of specific heats lower than that of air due to the exhaust composition. A possible alternative gas with a lower ratio of specific heats is carbon dioxide.

In-Cylinder Temperature

Figure 17 shows the peak in-cylinder temperatures for the pressurized motoring method using air and Argon, and the fired operation. The fired engine shows a temperature increase

FIGURE 17 The comparison of peak in-cylinder temperature between firing, motoring using air and motoring with Argon, at 1400 rpm

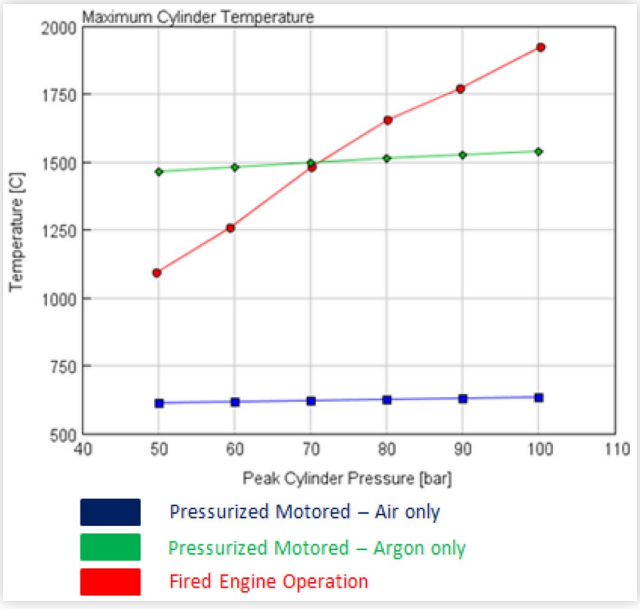

FIGURE 18 The comparison of in-cylinder temperature between firing, motoring with air, and motoring with Argon, at the same engine speed of 1400 rpm and PCP of 80 bar

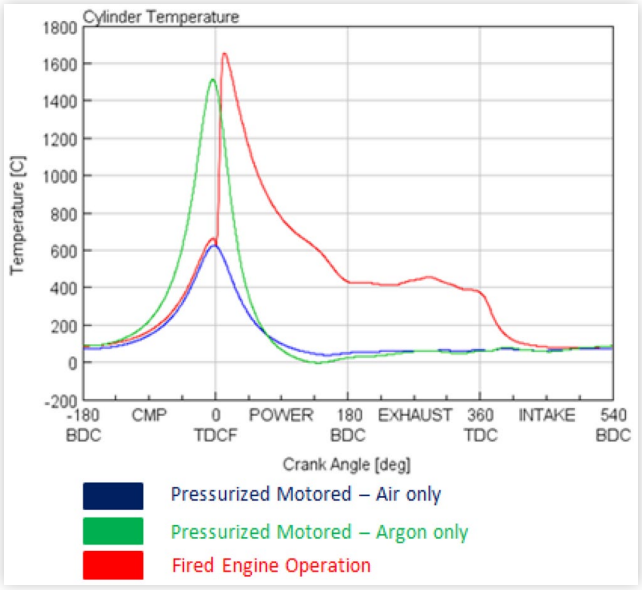

of around 750 °C from the 50 bar PCP to the 100 bar PCP. On the other hand, for both motoring methods (i.e. using air, and using Argon) the temperature is relatively constant, with that for Argon being considerably higher, and falling at the mid-range of the firing case. This quality of the pressurized motored method was already discussed in the previous section, and thought to be useful in obtaining a decoupling of the FMEP contribution due to the mechanical load and temperature. This quality is useful for understanding the FMEP dependency on temperature, particularly of new component designs. The ability of setting a temperature, which is relatively constant (with load and speed), but controllable by the experimentalist is the main benefit of using the Argon mixtures method. This ability is clearly not available with the fired indicating method.

To have a better understanding of the in-cylinder thermal conditions between the pressurized motoring using Argon and the fired engine, a 720 DegCA comparison of in-cylinder temperature is given in Figure 18. It is clear that even though the Argon testing manages to achieve peak in-cylinder temperatures close in magnitude to the fired case, however the crank angle resolved temperature is not identical to the fired temperature. Considering the compression stroke, it is seen that the Argon method induces a higher temperature than the fired operation. On the other hand, for the expansion stroke, the temperature of the Argon method is lower than the fired operation with a maximum discrepancy of around 750 °C.

The temperature observations hint that the Argon method might help achieve better representation in FMEP measurement around the TDC position, over the conventional pressurized motoring using air. However, it is understood that the Argon method is still prone to differences in the FMEP, particularly during the expansion stroke.

Heat Transfer

Figure 19 shows a comparison in the average heat transfer rates of the three methods. It is shown that the average heat transfer rate for the fired engine shows a large increase from the low PCP condition of 50 bar to the higher PCP condition of 100 bar. On the other hand, the pressurized motoring methods showed a very small increase in the average heat transfer rate. This is mainly derived from the earlier observation that bulk gas temperature in the pressurized motored engine is relatively constant for all PCPs and engine speed conditions.

Figure 19 also highlights the large heat transfer magnitude of the fired operation compared to both air and Argon pressurized motoring. This is due to the narrow angular range over which the pressurized motored in-cylinder bulk gas temperature increases. Furthermore, during this short angular range, the piston is close to the TDC position, meaning that the exposed liner area is very small. As a result, the average heat transfer rate for the pressurized motoring method is still relatively small, despite the high temperatures obtained.

Figure 20 shows the crank-angle resolved heat transfer rate for the pressurized motored setup using Argon, and the fired engine. The crank angle resolved heat transfer for pressurized motoring with air is left out for clarity. A rapid increase in the heat transfer rate occurs just after TDC for the firing condition. The Woschni sub-model calculates the heat transfer coefficient in terms of the cylinder geometry, the in-cylinder pressure, in-cylinder temperature, and piston velocity. For fired engine operation, the Woschni sub-model uses an additional term with the difference between the firing in-cylinder pressure and the in-cylinder pressure that would exist under motoring conditions. This pressure compensation term is not utilized for the operation of the engine at the pressurized motored condition, both conventionally using air, and also with Argon. Till the time of writing, only very small amount of experimental heat transfer data was obtained on the experimental engine run in the pressurized motored mode using Argon. Hence, verification of Figure 20, as computed from the Woschni sub-model is not yet possible.

FIGURE 19 The comparison of average heat transfer rate between firing, motoring using air and motoring with Argon, at the same engine speed of 1400 rpm.

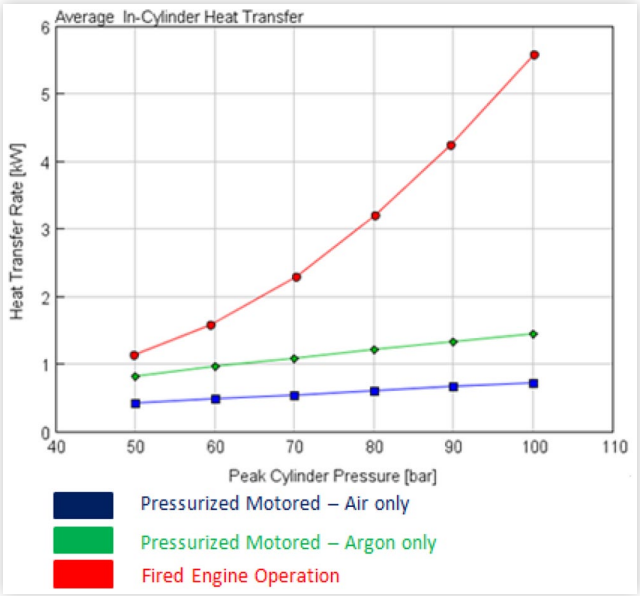

FIGURE 20 The comparison of in-cylinder heat transfer rate between firing and motoring with Argon, at the same engine speed of 1400 rpm and PCP of 80 bar

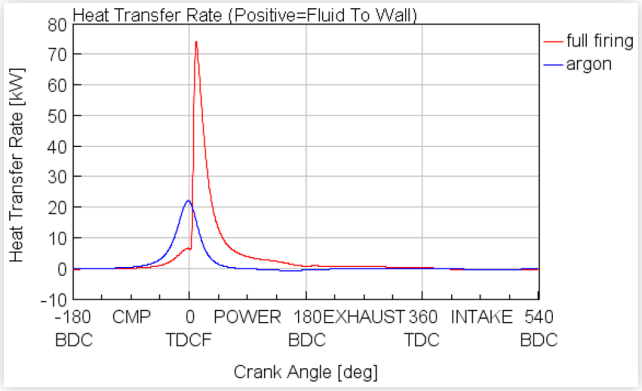

Indicated Mean Effective Pressure and FMEP Robustness Factor

The indicated mean effective pressure obtained for the pressurized motored and fired cases are given in Figure 21. It is evident that the IMEPnet for the Argon method has an overall larger magnitude than the pressurized motoring with air. This was already discussed in a previous section. Another observation is that the magnitudes for the pressurized motoring cases range between -1 bar at 50 bar PCP, and -3 bar at 100 bar PCP. On the other hand, for the fired case, the IMEPnet ranges between 2 bar at 50 bar PCP, and 12 bar at 100 bar PCP. It should be noted that utilizing a Chen-Flynn type correlation

FIGURE 21 The comparison of IMEPnet between firing, motoring using air and motoring with Argon, at the same engine speed of 1400 rpm

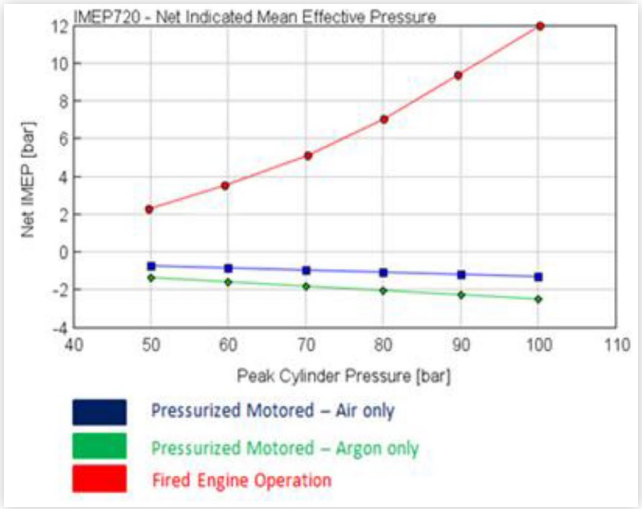

FIGURE 22 The comparison of FMEP robustness factor between firing, motoring using air and motoring with Argon, at the same engine speed of 1400 rpm

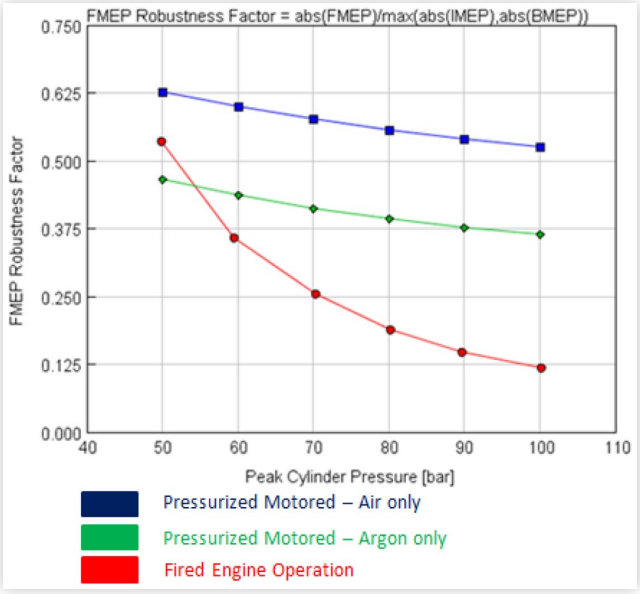

predicts identical FMEP between the two pressurized motoring cases and the fired case, since the PCP and engine speed were kept constant between the three methods.

For a given value of FMEP at a given PCP and engine speed, the FMEP robustness factor is significantly high for the pressurized motoring using air, slightly lower for the pressurized motoring using Argon, and very low for the fired engine, as shown in Figure 22. This shows the capability of the pressurized motoring methods to determine the FMEP with a much better accuracy than the fired engine (fired indicating method). It is noted that the FMEP robustness factor for the fired engine is relatively large for the low load conditions, but decreases to very small values at higher engine loads. On the other hand, for the pressurized motored methods, the FMEP robustness factor is fairly constant throughout the PCP range.

In the previous sections, the results obtained from the pressurized motoring using Argon at 1400 rpm were presented and discussed. A table with maximum and minimum values expected at the two extreme engine speeds was also given. A direct comparison was made between the pressurized motoring using Argon, pressurized motoring using air, and the fired engine at 1400 rpm and 80 bar.

While this publication showed that the Argon method gives the facility of adjusting the in-cylinder temperature independent of engine speed and load, it is clear that utilizing Argon does not yield a fired representative LPP. Hence the contribution on the FMEP due to pressure-to-crank angle phasing is not fully represented by this method. As a result, the authors presented an alternative novel method in [10], termed "Fuelled Pressurized Motoring" which was comprehensively described in the 'Introduction' section of this paper. In the following section, the fuelled pressurized motoring method is compared against the pressurized motoring with air and argon and the fired indicating method. The aim is to give the reader a broad view of the methods presented by this ongoing research, and how they distinguish themselves from one another.

Discussions

In this section a comparison between the FMEP determination methods studied so far by the authors is presented. Particular reference is made to the following methods:

1. Conventional motored tests (no manifold pressurization)
2. Pressurized motoring using air
3. Pressurized motoring using Argon/Air mixtures
4. Fuelled pressurized motoring (companion paper [10])
5. Fired indicating method

To aid understanding of the following comparison, Table 4 is given which grades the five methods in a relative manner. Since fuelled pressurized motoring is a relatively new

TABLE 4 A comparison on several criteria of interest between the discussed FMEP measurement methods

	Conventional Motoring	Pressurized Motoring Air Only	Pressurized Motoring Argon Mixtures	Fuelled Pressurized Motoring	Fired Indicating Method
Peak In-Cylinder Pressure Representation	✗	✓	✓	✓	Target
In-Cylinder Pressure Phasing Representation	✗	✗	✗	✓	Target
Peak In-Cylinder Temperature Representation	✗	✗	✓	✓	Target
Crank Angle Resolved Temperature Representation	✗	✗	✗	✓	Target
Representative Manifold Temperatures	✗	★	★	★★	Target
Pumping Losses Representation	★★	★	★★	★★	Target
Decoupling of FMEP contributors	★	★	★★	✗	✗
FMEP Robustness Factor	★★★★	★★★	★★	★★★★★	★
Testing Degree of Freedom	★	★★	★★★	★★★★	★★★★
Test Repeatability	★★	★★	★★	★	★
Simplicity of Test Setup	★★★★	★★★	★★	★	★★
Ease of Engine Test Control	★★★★★	★★★★	★★★	★	★★

method, to facilitate understanding of the forthcoming comparison, the reader is encouraged to revisit the relevant paragraph of the 'Introduction' section which describes in detail the fuelled pressurized motored method.

One of the main advantages of the pressurized motoring methods is the inherent simplicity and relatively low cost of running the FMEP tests. It was shown throughout this publication that for a 2.0 litre, single cylinder engine running at maximum speeds of 3000 rpm and maximum PCP of 160 bar, the brake power required to be supplied by the electric motor does not exceed 8 kW. This was obtained through simulation results that are in agreement with measurements obtained experimentally, and presented earlier. Coupled to the ability of running the engine at very small gas supply flow rates gives a very desirable test combination. Testing simplicity is somewhat decreased for the fuelled pressurized motored method due to the addition of small fuel injections which present two additional control variables to the test matrix. Another advantage of the pressurized motored methods over the fuelled pressurized motoring and the fired indicating method is that the absence of combustion results in lower COVs, and hence a more repeatable FMEP.

The pressurized motoring methods present the characteristic of a relatively constant in-cylinder temperature at the different engine speeds and PCPs. This allows decoupling of the FMEP contributions from engine speed, mechanical load and thermal conditions. This quality is particularly useful in determining the individual FMEP contributions of the engine speed, mechanical load, and bulk gas temperature independently. For example, it can be used to assess the FMEP characteristics of alternative piston-to-bore clearances, piston pin offset and coating, width and tension of piston rings, engine oil viscosity, piston skirt profile, roughness, coating, area and stiffness [1]. Utilizing the Argon method gives the additional advantage that the in-cylinder temperature (constant with speed and PCP) can be controlled by the experimentalist from low motoring values to high fired values, by increasing the Argon mass concentration. The fired indicating method, and also the fuelled pressurized motoring method are not able to present this decoupling effect between the three major FMEP contributors. However the fuelled pressurized motored method shows through simulation a better thermal representation of the fired engine, when compared to the Argon method as shown in Figure 23. This is due to the ability of the fuelled pressurized motoring to emulate high gas temperatures during the expansion stroke; something which the Argon method is not capable of.

Even though the fuelled pressurized motoring method is thought to have a better capability than the Argon method in emulating the in-cylinder temperature of the fired engine, it should be understood that to achieve this, some trade-off must be made on FMEP robustness factor and other metrics. It should also be clear that the fuelled pressurized motoring does not provide the benefit of having a constant in-cylinder temperature at different speeds and different loads, as proved achievable by the Argon mixtures. In view of this, it is thought that the fuelled pressurized motoring and the pressurized motoring using Argon are not two rival methods, but actually

FIGURE 23 The graph of in-cylinder temperature against crank angle for the different FMEP methods.

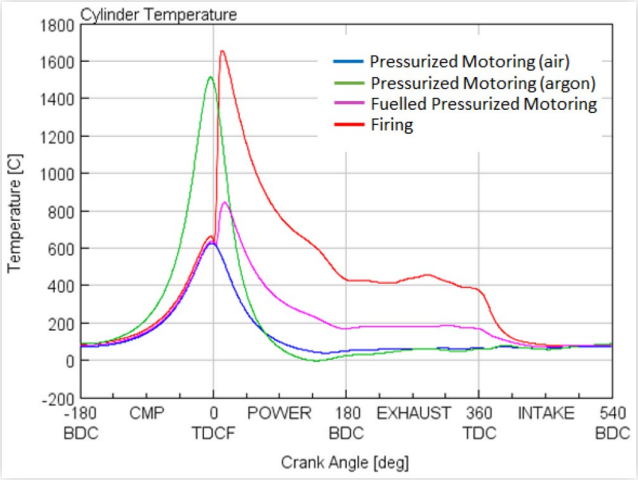

two methods which aim to provide two different solutions. The fuelled pressurized motoring allows the measurement of the FMEP at very good representation of the fired engine. On the other hand, the pressurized motoring using Argon allows FMEP measurement with the possibility of decoupling the contribution of engine speed and mechanical load from the in-cylinder temperature; which can be controlled by the experimenter from low motored magnitudes to high fired magnitudes.

A metric known as 'FMEP Robustness Factor' was introduced previously to gauge the ability of the method in determining an accurate FMEP measurement. The higher the FMEP robustness factor, the lower is the uncertainty propagation. It was shown that the pressurized motoring using air already provides a very good FMEP robustness factor since the BMEP and IMEP are both comparable in magnitude to the FMEP. The FMEP robustness factor for the fired indicating method (fired engine) is unfortunately very low, even though this method gives the best representation of FMEP. The pressurized motoring using Argon seems to fall between the two methods, where the FMEP robustness factor is better than that for the fired indicating method, but not as good as that for the pressurized motoring with air. This originates from the fact that the IMEP with Argon has larger values than the IMEP with air due to a higher magnitude of heat losses. As a result this deteriorates slightly the performance of the method in the FMEP robustness, as a trade-off for obtaining a higher in-cylinder temperature. The fuelled pressurized motoring showed in [10] the ability of obtaining the highest achievable FMEP robustness factor, which can reach values as high as 2.0. This mainly results from the ability of varying the IMEP from small negative values to small positive values, by controlling the injection strategy. The FMEP robustness factor for the Fuelled Pressurized Motoring is compared with those for the other methods and shown in Figure 24. Note that in generating Figure 24 in GT suite, the fuelled pressurized motored method was not run with the aim of obtaining the highest FMEP robustness factor. Hence the values shown in

FIGURE 24 The FMEP robustness factor for the different FMEP methods.

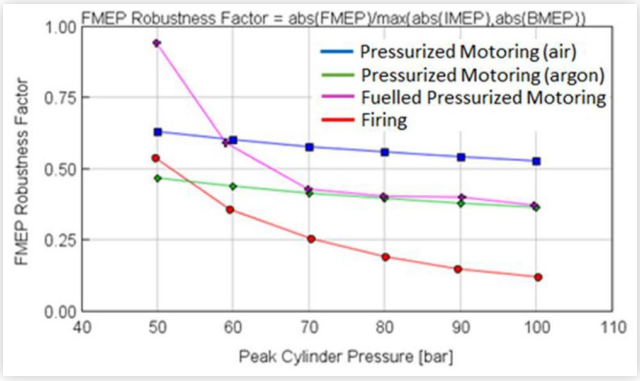

Figure 24 are only indicative. Higher FMEP robustness factors (up to around 2.0) can be achieved with the fuelled pressurized motored method.

All of the pressurized motored methods showed to be capable of reaching a peak in-cylinder pressure close to that of the fired engine. Phasing of the pressure with crank angle was however different for each method, as shown in Figure 25. The fired operating condition, which is the benchmark condition, shows an LPP of around 10 DegCA ATDC for CI engines (and up to around 20 DegCA ATDC for SI engines, which are not discussed in this paper but a benchmark value is worth mentioning). The pressurized motoring with air presents a relatively constant LPP at around 1 DegCA BTDC [2] [7]. Argon advances further the LPP prior to TDC. The fuelled pressurized motored method [10] showed the ability of achieving LPPs ranging from 1 DegCA BTDC up to around 9 - 10 DegCA ATDC. LPP is a convenient indicator of the pressure phasing with crank angle. In FMEP studies, pressure phasing is considered of utmost importance, as this determines the magnitude of the piston lateral thrust, and hence directly affects the FMEP.

FIGURE 25 The LPP for the different FMEP methods.

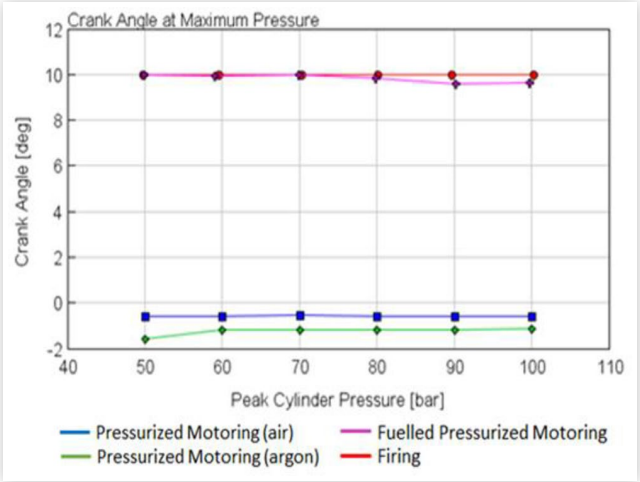

Application of FMEP Experimental Data to Sub-Models

The pressurized motoring method is an FMEP determination method which, at present, is in competition with methods like the teardown test, fired indicating method, conventional motoring and Morse test. These are methods which are known to provide less than adequate FMEP measurements originating from largely unrepresentative FMEP, large error propagations, and high cycle-to-cycle variability. As a consequence of the lack of reliable experimental FMEP data, FMEP models representative of modern, highly optimized engines are few, with the more common engine simulation software still making use of the Chen-Flynn type correlation. This publication, along with the previously published work in [7], [8], [9] and the companion paper [10] aims to develop further the pressurized motoring method. This method was chosen as the basis for improvement due to its high repeatability, high robustness factor, and moderate fired-engine representation. It is acknowledged that this method, even with the use of Argon (and small fuel injections, as in [10]) is still not able to fully reach the ultimate aim, i.e. to have a fully representative FMEP method with the highest possible FMEP robustness factor. However, it is thought that at present this method offers a very competitive balance between FMEP robustness, fired-engine representation and ease of implementation.

Conclusions

In this publication, a simulation study was conducted using GT suite. A correlation of the simulation with the experimental data presented in [8] and [9] was presented for the engine utilizing Argon mixtures. Results showed that the simulation is capable of capturing several observations which were seen in the experimental research by the same authors, using the same 2.0 litre engine. On the other hand, the Chen-Flynn type FMEP sub-model was shown to be unable to distinguish between pressurized motored operation and fired operation, since it is sensitive only to engine speed and PCP. No account is taken for the FMEP sensitivity to pressure load - piston velocity phase relationship, and in-cylinder temperatures. This is considered as one of the weak points in engine simulation at present, and it is one of the aims of this work, i.e. to help provide an experimental method which can supply reliable and representative FMEP data for novel FMEP model development. At present, FMEP models range between the simple Chen-Flynn type which utilizes just one value of in-cylinder pressure (i.e. PCP) to very complex FMEP models which are able to consider bore distortion, ring tension, and other complex mechanisms, which makes their use in engine design optimization time consuming and costly. It is thought that a fair compromise can be reached between these two extremities by an FMEP model which utilizes the whole in-cylinder pressure cycle as an input.

The Woschni derived sub-model used for the prediction of the heat transfer rate determination showed that the

pressurized motoring engine using Argon experiences a much lower average heat transfer rate when compared to the average heat transfer rate for the fired engine. This observation could not be compared to experimental results, as sufficient heat transfer rate experimental data using Argon is not yet available.

Based on an observation made on the in-cylinder temperature, it was understood that even though high peak in-cylinder temperatures are reached with the use of Argon, however the temperature on the expansion stroke is still not fully representative of the actual fired engine. This might induce some discrepancy in the FMEP between firing and pressurized motoring. Despite this, it is appreciated that the Argon method has the unique capability of decoupling the FMEP contribution from the engine speed, mechanical load, and temperature, which is beneficial, especially for analyzing FMEP contribution of new component designs [1]. Use of Argon-air mixtures presented the added advantage that the constant in-cylinder temperature (with engine speed and PCP) can be varied and controlled independently by varying the Argon mass concentration. Hence it allows the decoupling of the FMEP contribution, but also allows an analysis of the FMEP variation with temperature.

The FMEP robustness factor was shown to degrade slightly with the use of Argon due to having higher heat losses, which result in a slight increase in the IMEP magnitude. Despite this, the value of the FMEP robustness is still much better than that of the fired engine, and hence it is thought that the trade-off on the FMEP robustness is leveraged by the higher in-cylinder temperatures which allow better fired engine representation.

Suggestions for Further Work

At the time of writing, the experimental pressurized motored single cylinder engine is being instrumented with surface thermocouples in the aim of extending the study into the heat transfer phenomena occurring in the pressurized motored engine. It is hoped that this data will be able to provide adequate basis against which quasi-steady heat transfer models, such as the Woschni-type can be compared.

To strengthen further the method brought forward here and in the companion paper [10], experiments on different engine geometries, at higher engine speeds, higher mechanical loads, and different oil and coolant temperatures can be made. These factors should be able to give a good ground over which novel FMEP models can be based.

References

1. MAHLE International GmbH, "Engine Testing," in *Pistons and Engine Testing* (Stuttgart, Germany: Springer), ch. 7, 117-281.
2. Mauke, D., Dolt, R., Stadler, J., Huttinger, K. et al., *Methods of Measuring Friction under Motored Conditions with External Charging* (Switzerland: Kistler Group, 2016).
3. Richardson, D.E., "Review of Power Cylinder Friction for Diesel Engines," *Transactions of the ASME* 122, 2000.
4. Allmaier, H. et al., "An Experimental Study of the Load and Heat Influence from Combustion on Engine Friction," *International Journal of Engine Research* 17(3):347-353, Mar. 2015.
5. Ullmann, K., *Die mechanischen Verluste des schnellaufenden Dieselmotors und ihre Ermittlung mit dem Schleppversuch* (Berlin: VDI-Verlag GmbH, 1939).
6. Pike, W.C., and Spillman, D.T., "The Use of a Motored Engine to Study Piston-Ring Wear and Engine Friction," *Proceedings of the Institution of Mechanical Engineers* 178(14):37-44, 1963.
7. Caruana, C., Farrugia, M., Sammut, G., and Pipitone, E., "Further Experimental Investigation of Motored Engine Friction Using Shunt Pipe Method," SAE Technical Paper 2019-01-0930, 2019, https://doi.org/10.4271/2019-01-0930.
8. Caruana, C., Pipitone, E., Farrugia, M., and Sammut, G., "Experimental Investigation on the Use of Argon to Improve FMEP Determination through Motoring Method," SAE Technical Paper 2019-24-0141, 2019, https://doi.org/10.4271/2019-24-0141.
9. Caruana, C., Farrugia, M., Sammut, G., and Pipitone, E., "Further Experiments on the Effect of Bulk In-Cylinder Temperature in the Pressurized Motoring Setup Using Argon Mixtures," SAE Technical Paper 2020-01-1063, 2020, https://doi.org/10.4271/2020-01-1063.
10. Sammut, G., Farrugia, M., Pipitone, E., and Caruana, C., "A Simulation Study Assessing the Viability of Shifting the Location of Peak In-Cylinder Pressure in Motored Experiments," SAE Technical Paper 2020-24-0009, 2020, https://doi.org/10.4271/2020-24-0009.
11. Caruana, C., Farrugia, M., and Sammut, G., "The Determination of Motored Engine Friction by Use of Pressurized 'Shunt' Pipe between Exhaust and Intake Manifolds," SAE Technical Paper 2018-01-0121, 2018, https://doi.org/10.4271/2018-01-0121.
12. Caruana, C., Farrugia, M., Sammut, G., and Pipitone, E., "One-Dimensional Simulation of the Pressurized Motoring Method: Friction, Blow-by, Temperatures and Heat Transfer Analysis," in *IMECHE - Internal Combustion Engines and Powertrain Systems for Future Transport*, West Midlands, Birmingham, Dec. 11-12, 2019.
13. Gamma Technologies, "GT-Power User's Manual," 2017.
14. Camilleri, S., "Investigation of Common Rail Diesel Engine," University of Malta, Msida, Undergraduate Dissertation, 2011.
15. Demuynck, J. et al., "Applying Design of Experiments to Determine the Effect of Gas Properties on In-Cylinder Heat Flux in a Motored SI Engine," *SAE Int. J. Engines* 5(3), 2012.
16. Finol, C.A., and Robinson, K., "Thermal Modelling of Modern Engines: a Review of Empirical Correlations to Estimate the In-Cylinder Heat Transfer Coefficient," *Proceedings of the Institution of Mechanical Engineers, Part D: Journal of Automobile Engineering* 220(12):1765-1781, Dec. 2006.
17. Pipitone, E., and Beccari, A., "Determination of TDC in Internal Combustion Engines by a Newly Developed Thermodynamic Approach," *Applied Thermal Engineering* 1914-1926, 2010.

Contact Information

Gilbert Sammut
Jaguar and Land Rover
gsammut@jaguarlandrover.com

Mario Farrugia,
Mechanical Engineering Department,
University of Malta, Malta,
mario.a.farrugia@um.edu.mt

Acknowledgments

The research work disclosed in this publication is partially funded by the Endeavour Scholarship Scheme (Malta). Scholarships are part-financed by the European Union-European Social Fund (ESF)-Operational Programme II-Cohesion Policy 2014-2020 "Investing in human capital to create more opportunities and promote the well-being of society".

Definitions/Abbreviations

ATDC - After Top Dead Centre
BBDC - Before Bottom Dead Centre
BDC - Bottom Dead Centre
BMEP - Brake Mean Effective Pressure
BTDC - Before Top Dead Centre
CAD - Crank Angle Degrees
CI - Compression Ignition
COV - Coefficient of Variation
EVO - Exhaust Valve Opened
FMEP - Friction Mean Effective Pressure
HDi - High-Pressure Direct Injection
IMEP - Indicated Mean Effective Pressure
IVC - Intake Valve Closed
LPP - Location of Peak In-Cylinder Pressure
MAP - Manifold Absolute Pressure
OEM - Original Equipment Manufacturer
PCP - Magnitude of Peak In-Cylinder Pressure
PMEP - Pumping Mean Effective Pressure
TDC - Top Dead Centre

ISSN 0148-7191